Optical Fiber Spectroscopy: A Study of the Luminescent Properties of the Europium Ion for Thermal Sensors

Annual Report for NASA Grant NAG 1-1443
National Aeronautics and Space Administration
Langley Research Center
Hampton, Virginia

Submitted to
Dr. Robert S. Rogowski, Technical Monitor
Mail Stop 231

Submitted by
A.Martin Buoncristiani
Department of Physics and Computer Science
Christopher Newport University
Newport News, Virginia
23606

INTRODUCTION

Recently, there has been interest in developing a distributed temperature sensor integrated into an optical fiber. Such a system would allow embedding of the optical fiber within or on a structural material to provide for continuous monitoring of the material's temperature [1-7]. Work has already begun on the development of a temperature sensor using the temperature dependent emission spectra from the lanthanide rare earths doped into crystalline hosts. The lifetime, the linewidth and the integrated intensity of this emission are each sensitive to changes in the temperature and can provide a basis for thermometry. One concept for incorporating this phenomena into an optical fiber based sensor involves bonding the optically active material to the cladding of an optical fiber and allowing the luminescent light to couple into the the fiber by the evanescent wave [6]. Experimental work developing this concept has already been reported [7]. Measurements of the linewidth of Eu^{3+}: Y_2O_3 , diffused into a fiber,made by Albin clearly show a strong and regular dependence on temperature over the range of 300 to 1000 K [2,4].

We report here on a study of the temperature dependence of the lineshape of the emission at 611 nm using the data in references [2, 9-12]. We focus attention on understanding the general behavior of the Eu^{3+}: Y_2O_3 system. Building upon understanding of this system we will be able to establish the physical criterial for a good optical fiber based temperature sensor and then to examine available data on other lanthanide rare earths and transition metal ions to determine the best luminescent system for temperature sensing in an optical fiber.

LUMINESCENCE OF Eu^{3+}: Y_2O_3

The Y_2O_3 crystal has a cubic structure with unit cell dimension 10.61 Å [10]. Each yttrium ion has six oxygen ions as nearest neighbors configured to occupy six of the eight corners of a cube surrounding the yttrium ion. There are two distinct arrangements of the oxygen around each yttrium site. In one arrangement the two vacant oxygen sites are at opposite diagonals of the cube forming a high symmetry (centro-symmetric) site of symmetry C_{3i} ; in the other arrangement the oxygen vacancies are at opposite diagonals of a cube face forming a low symmetry site of symmetry C_s. The triply ionized Europium ion is in a $4f^6$ electron configuration and substitutes for the triply ionized Yttrium ion in either of these two distinct crystallographic sites. There are three of the low symmetry C_s sites for each C_{3i} site. A Europium ion at a C_s site will have its degeneracy fully broken but it will be only partially broken in the C_{3i} site. The energy levels and Stark splittings for Eu^{3+}:Y_2O_3 are well known and correspond to theoretical predictions [8,9]. The Stark levels for the low lying energy manifolds relevant to this discussion are listed in Table 1.

Table 1.
Stark Levels of the ^7F_J and ^5D_J Manifolds of Eu^{3+}: Y_2O_3
(Only the energy levels for the Cs symmetry sites are listed)
(from references 8 and 9)

Manifold	Energy level (cm^{-1})
$^7F_0$	0
$^7F_1$	199, 369, 543
$^7F_2$	859, 906, 1379
$^7F_3$	1847, 1867, 1907, 2008, 2021, 2130, 2160
$^7F_4$	2668, 2800, 2846, 3015, 3080, 3119, 3163, 3178, 3190
$^7F_5$	3755, 3828, 3904, 3938, 4019, 4062, 4127, 4158, 4227
$^7F_6$	4589, 4611, 4791, 4812, 4925, 4960, 5032, 5045, 5271, 5314, 5459, 5636
$^5D_0$	17216
$^5D_1$	18930, 18954
$^5D_2$	21355, 21357, 21396

Our discussion is focused on the characteristics of luminescence in the region of 611 nm; the possible transitions between Stark levels that could contribute to this luminescence are listed in Table 2.

Table 2.
Transitions Contributing to Luminescence near 611 nm

Manifold	Transition Wavelength (nm)
$^5D_0 \rightarrow ^7F_2$	611.36, 613.12
$^5D_2 \rightarrow ^7F_6$	609.42, 612.63, 613.12
$^5D_2 \rightarrow ^7F_6$	612.56, 613.05
$^5D_2 \rightarrow ^7F_6$	611.10, 611.58

The radiative transitions between the between $^5D_2 \rightarrow ^7F_6$ manifolds are strongly quenched above room temperature so they would not be expected to contribute the high temperature luminescence; this has been demonstrated by Klassen et al. [11]. On the other hand one can expect contributions

from both of the Stark level transitions connecting the $^5D_0$ -->$^7F_2$ manifolds. For the C_S symmetry sites, there are three major Stark levels in the $^7F_2$ manifold and one in the $^5D_0$ manifold; these contribute to emission at 611.36, 613.12 and 631.4 nm. As shown in sequel, the assymetry observed in the spectral shape of the emission near 611 nm line is due to the combined emission from the nearby transitions at 611.36 and 613.12 nm. There may be additional contributions to this lineshape from phonon sidebands, however these are not expecrted to be large since the vibronic coupling to the Y_2O_3 lattice has been shown to be weak both theoretically [9] and experimentally [11].

Albin has measured the emission spectra of Eu^{3+}: Y_2O_3 in the region of 611nm at temperatures ranging from 323 K to 973 K. These measurements were made on powdered samples thermally diffused into an optical fiber which was used to collect the emitted light. The temperature dependence of the linewidth extracted from these spectra is shown in Figure 1. The raw data is fit to a quadratic expression in temperature. In the following we develop a model for this temperature dependence.

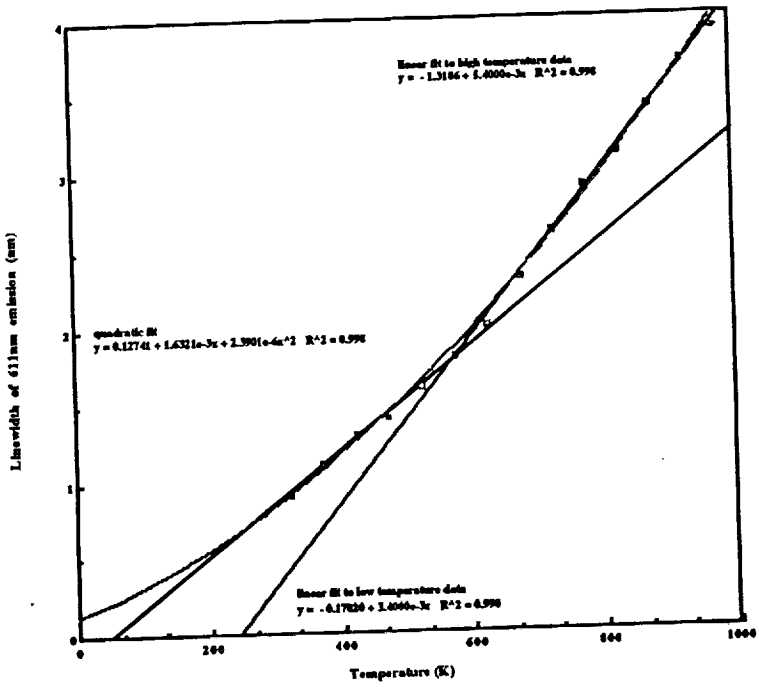

Figure 1. Measured values of the linewidth of the 611 nm emission of Eu^{3+}: Y_2O_3 from Albin, reference [5]. Curves indicate a quadratic fit to the data and linear regression fitting to the low and high temperature regions separately.

THE Eu^{3+} LUMINESCENCE CENTER

The basic phenomena responsible for the temperature dependence of the spectral shape of the luminescence at temperatures above room temperature can be understood by considering emission from a single prototypical Eu^{3+} luminescent center [12, 14]. Both the radiative and non-radiative processes that take place at a luminescent center can be described by a single configuration coordinate which treats all of the vibrational components of each energy level of the optically active ion as an harmonic oscillator. Levels connected by phonon assisted electronic transitions are each represented by parabolic simple harmonic oscillator potentials displaced along the single configuration coordinate as shown in Figure 2. Assuming that the force constants for each harmonic parabola are equal, the two parabolic energy surfaces can be described by the following expressions

$$E_l = \frac{1}{2} kq^2 = S_l \bar{h}\omega \left(\frac{q}{a}\right)^2 \qquad (1)$$

and

$$E_u = E_{zp} + S_u \bar{h}\omega \left(\frac{q - a}{a}\right)^2 \qquad (2)$$

Where q represents the configuration coordinate and E_l and E_u refer to the electronic energies of the ground state and excited state respectively. The two parabolas are offset by a distance a. S_u and S_l are the number of phonons at emission and absorption center (the Huang-Rees parameters). E_{zp} represents the zero phonon energy

The occupation probability for the n^{th} vibrational state of a given manifold is given by

$$P(n,z) = (1 - z)\, z^n \qquad (3)$$

where,

$$z = e^{-\bar{h}\omega/kT}.$$

The emision of a photon with energy hν can occur between the excited state with vibronic quantum number l and the ground state with vibronic quantum number m, where

$$p = \frac{h\nu - E_{zp}}{\bar{h}\omega} = (l - m)$$

represents the number of phonons involved in the transition. The normalized linestrength is given by the sum over Frank-Condon factors

$$W_p = \sum_{m = \max\{0,-p\}}^{\infty} P(m,z) \langle l_{p+m} | u_m \rangle \qquad (4).$$

Non-radiative rates can be determined from the same sum over Frank-Condon factors and the electronic transition rate $R_{electronic}$ as $R_p = R_{electronic} W_p$. In general, it is not expected that the vibronic levels will have the same force constants but the description above illustrate how a simple lineshape can be re-constructed.

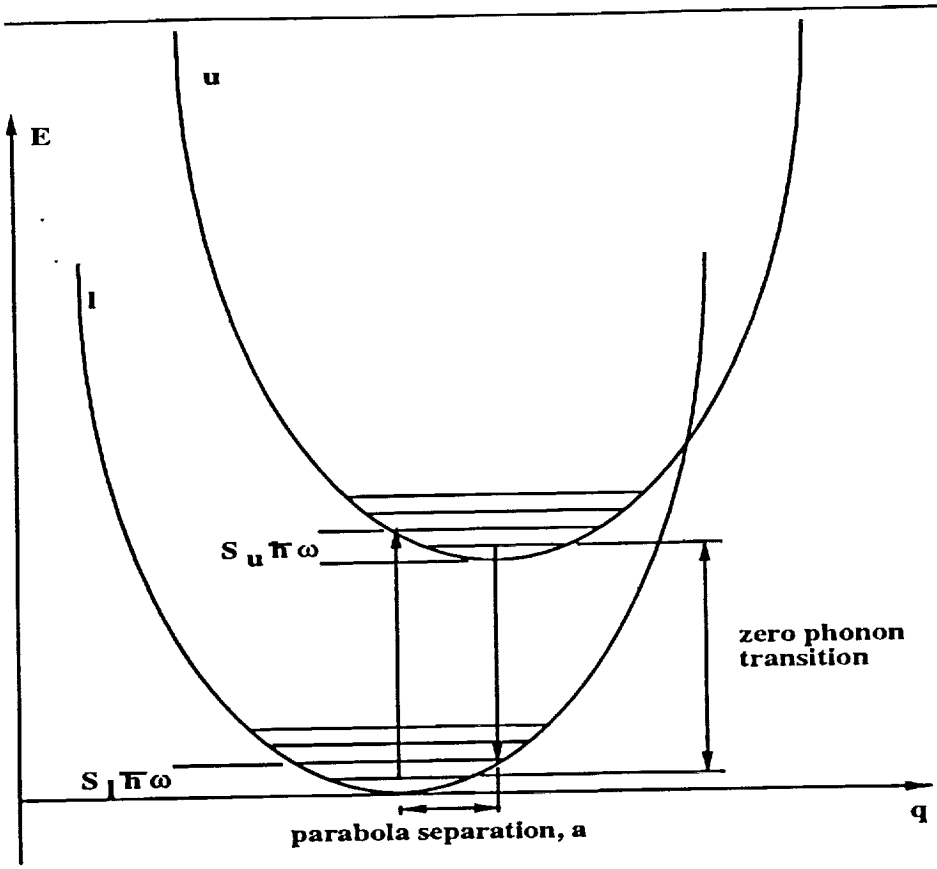

Figure 2. Representation of the vibrational and electronic energy levels of a luminescence center in terms of the configuration coordinate.

LINE BROADENING MECHANISMS

Several different physical mechanisms may contribute to the broadening of the narrow line emission of the lanthanide rare earths doped into activated crystals [14,15]:

a) There is an inhomogeneous component to the linewidth due to the fact that the dopant ions experience slightly different microstrains at each impurity site. These strains are randomly distributed and they produce a gaussian lineshape that is only weakly temperature dependent. However this strain broadening is especially critical for this application which may employ Eu^{3+}: Y_2O_3 powder on the exterior of a fiber.

b) There is a contribution due to Raman scattering of phonons by the impurity ions. This contribution depends upon the Debye temperature of the host T_D and the strength of the coupling between the impurity ion and the lattice.

c) There is a contribution due to single phonon emission and absorption which depends upon a separate electron-phonon interaction parameter.

d) There also may be a contribution from anharmonic interactions between the impurity ion and the lattice resulting in local (non-propagating) modes.

We have estimated the size of the most important of these effects in order to get an idea of the cause of the observed temperature dependence of the lineshape.

Frank-Condon Lineshape

First we make a simple arguement for the variation of the linewidth with temperature based solely on the shape of the harmonic potential in a single configuration coordinate model (the Frank-Condon factor). At zero temperature the lineshape, in the Condon approximation, is a Gaussian with linewidth proportional to the amplitude of the zero point oscillations of the excited state. As temperature rises, higher energy vibrational levels become populated and the corresponding wavefunctions extend further in configuration coordinate space. The increase in linewidth should be proportional to this extension of the wavefunction, that is, proportional to the amplitude of a classical oscillator. The zero point amplitude of a harmonic oscillator with vibrational (phonon) energy E_p is given by

$$A_0^2 = E_p/k \,, \tag{5}$$

where k is the Boltzmann constant. The amplitude of the nth quantum energy level is related to the zero point amplitude by

$$A_n^2 = (2n + 1)A_0^2 .$$

The temperature dependence of the linewidth is obtained by summing over the amplitudes of all harmonic oscillator energy levels, weighted by the probability of their occupancy

$$\langle A \rangle^2 = \frac{\sum_{n=0}^{\infty} e^{-n\, h\nu/kT}\ A_n^2}{\sum_{n=0}^{\infty} e^{-n\, h\nu/kT}} \,, \tag{6}$$

and this leads to the following experssion for the temperature dependence of linewidth

$$\Delta\nu(T) = \Delta\nu(0)\,(\tanh(E_p/2kT))^{-\frac{1}{2}} . \tag{7}$$

This equation describes the change in linewidth due only to temperature induced changes in the occupation probability of the harmonic energy levels associated with the excited state. Figure3 shows the temperature dependence of the linewidth predicted by Equation 7 for various values of phonon energy, E_p with the measured values of linewidth are superimposed. Clearly the measured linewidth increases more rapidly with temperature than Equation (7) predicts. This indicates that the lineshape is not determined by the single configuration coordinate picture alone but that other processes are at work. In the following paragraph we show that the steep change in linewidth with temperature can be explained by including the effect of a second nearby Stark level transition. If we

force a fit of the measured data to Equation 7 we obtain an unreasonable small value of phonon energy equal to 0.2 meV (1.6 cm^{-1}).

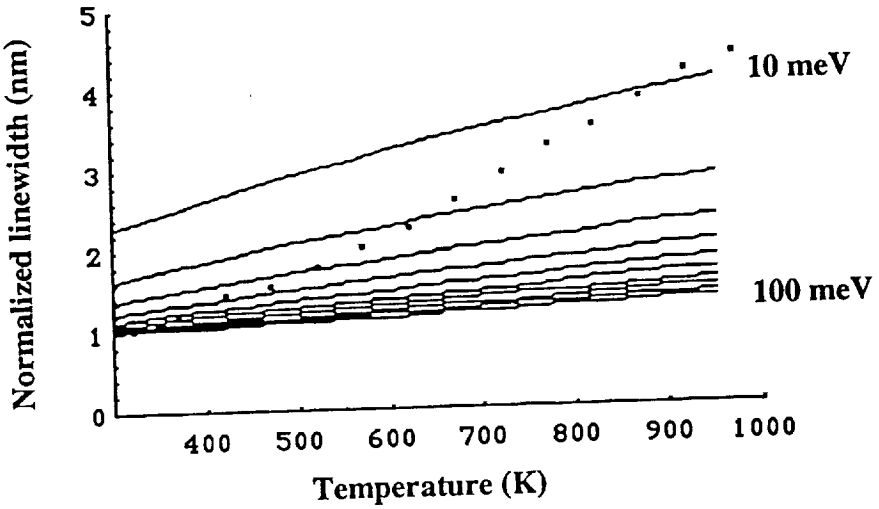

Figure 3 The change in linewidth with temperature as predicted by the broadening of the vibronic potential energy curve, Equation 7. Superimposed upon these curves are the data from reference 5 normalized to unity at the lowest temperature measured.

Two level Frank-Condon Lineshape

As Figure 3 indicates, the measured linewidth rises much faster than predicted by the broadening of the configuration coordinate potential curve, Equation 7. One possible source for an additional contribution to linewidth can come from the emission from a second Stark level transition close to the 611.36 nm line. From Table 2 we see that there is a $^5D_0$ --> $^7F_2$ transition at 613.12 nm which can contribute to emission at 611 nm. To test this idea we calculate the emission from both of these Stark level transitions. We assume that each line has a Lorentz lineshape which changes with temperature according to the Frank-Condon linewidth factor given in Equation 7. Thus the lineshape depends upon the phonon energy Ep and intrinsic linewidth $\Delta\lambda$ for each transition. The strength of the transition can be calculated from W_p given by Equation (4) with p taken to be zero. We use p equal to zero because the separation between the two lines (56.8 cm^{-1}) is much smaller than the maximum phonon wavelength for Y_2O_3 (about 550 cm^{-1}).

The results of this calculation of the lineshape for the 611 nm emission are shown in Figure 4 for two values of temperature.The results are in good quantitve agreement with both the general shape of the emission line and its change with temperature. It is difficult to render a accurating fitting with the small amount of data available. However, the qualitaitive agreement does suggest that other mechanisms can influnece the temperature dependence of emission and that these enhnacements may provide the basis for sensitive temperature sensors. Mechanisms which can provide such enhancements include the cooperative emission from two close Stark level transitions, thermal

quenching of manifolds which feed the manifold under observation and thermal equilibrium set up by energy transfer between manifolds.

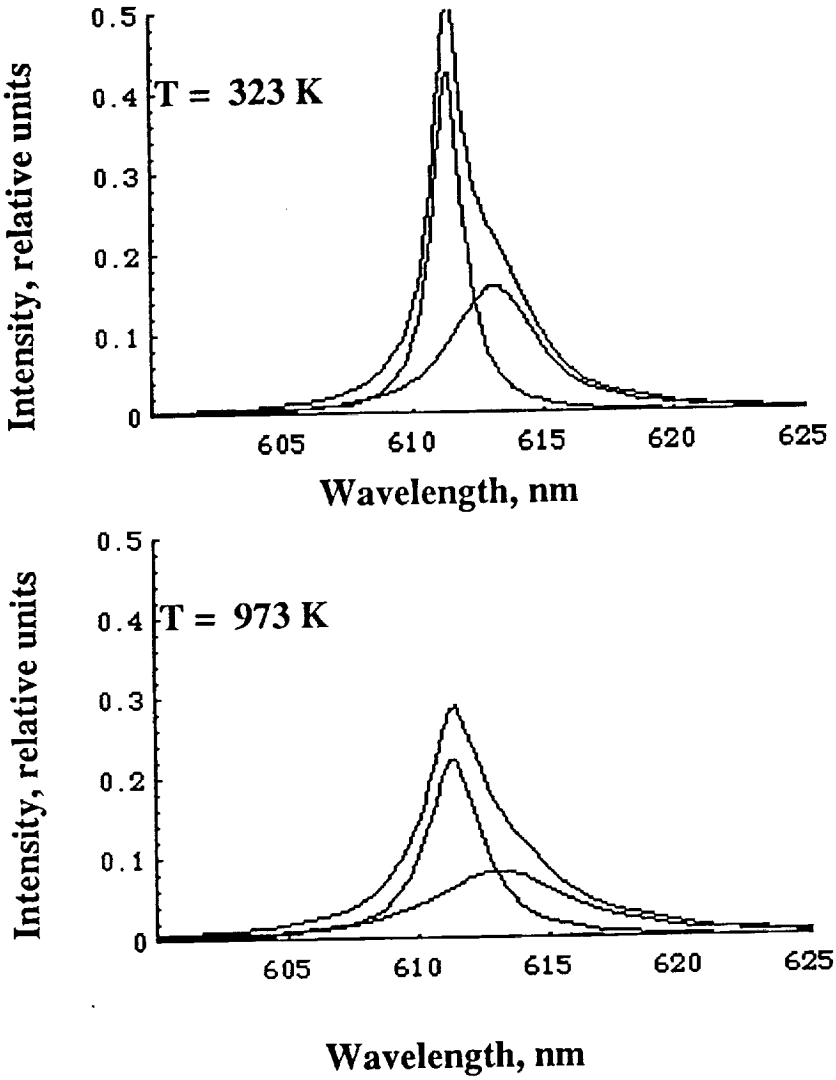

Figure 4. The calculated lineshape for the 611 nm emission assuming that two nearby Stark level transitions (611.36 nm and 613.12 nm) contribute. Each level has a Lorentz lineshape which changes with temperature according to the Frank-Condon factor (Equation 7).

Single phonon linewidth

The previous calculations assumed that a single phonon energy E_p was available to broaden the electronic transitions but that many of these phonons of this energy could participate in the transition. We now consider a process involving a single phonon of energy $\hbar\omega$ to calculate the temperature dependence of the linewidth of the 611.4 nm emission. We can fit the measured

linewidth using a model of the electron-phonon interaction involving single phonon processes. From McCumber and Sturge [12] the single phonon contribution to linewidth has the form

$$\Delta\nu_{\text{phonon}} = \frac{|C_{12}|^2}{2\pi}\frac{V}{v^5}\omega^3\left(e^{\hbar\omega/kT}-1\right)^{-1},$$

where C_{12} is the matrix element for the transition and gives the strength of the electron-phonon coupling, V is the volume of the crystal, v is its speed of sound (assuming the transverse and longitudinal speeds are equal), and $\hbar\omega$ is the single phonon energy.

The data taken by Albin can be fit to the following expression,

$$\Delta\nu = a + b\,\omega^3\,(\exp(\hbar\omega/kT) - 1)^{-1}. \qquad (8)$$

with a = 0.0434, b = 0.0000135 and $E_p = \hbar\omega = 68.7$ meV (554 cm^{-1}). The single phonon energy is within the phonon spectrum for this host and is in fact close to the value found in Reference 11 for the phonon responsible for quenching the ^5D_J manifolds. This fit to Albin's data is shown in Figure 5. This fit is very good.

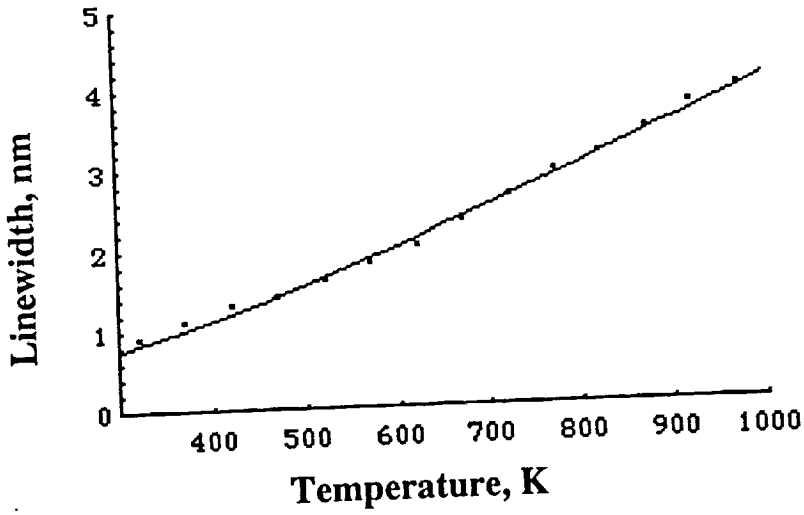

Figure 5. Fit of the linewidth data from Reference 2 to Equation 8.

CONCLUSIONS

We have initiated a study of rare earth luminescence as part of an effort by NASA to develop a temperature sensor that can be integrated into a optical fiber. This report focuses on luminescence from Eu^{3+}:Y_2O_3 We have described the physical characteristics of the Y_2O_3 crystalline host and the Eu^{3+} luminescence center. We have examined the temperature dependence of the linewidth of the 611 nm luminescence from Eu^{3+}:Y_2O_3 obtained from powder thermally diffused into a fiber measured by Albin [2]. The temperature dependence of the the 611nm luminescence was shown to be stronger than that expected from the Frank-Condon principle alone. The temperature dependence of the lineshape can be qualitatively explained by a model using emission from two nearby transitions. A good fit to the measured temperatue dependence of linewidth is obtained using a single phonon model.

The observation that the temperature dependence of linewidth is more rapid than expected from a Frank-Condon model and the conjecture that some combined emission is responsible for this enhanced dependence suggests that there may be other instances of enhanced emission that would be useful in sensing. Such mechanisms include the cooperative emission from two close Stark level transitions, thermal quenching of the manifolds which feed the manifold under observation and thermal equilibrium set up by energy transfer between manifolds. A fruitful line of investigation would be to search the rare earth energy levels for patterns that might give such enhanced emission.

REFERENCES

[1] E. Udd, Fiber Optic Sensors, John Wiley and Sons, Inc (1991).

[2] S.Albin, Temperature Sensors Based on Stimulated Emission of Doped Optical Fibers, Contract Report: Master Contract NAS1-18584, March (1992).

[3] A.M.Buoncristiani, Solid State Lasers for Use in Non-contact Temperature Measurements, Proc. 2 nd Non Contact Temperature Measurement Workshop, JPL Publication 89-16, pp. 60-69 (1989).

[4] A.R.Bugos, S.W.Allison, D.L.Beshears and M.R.Cates, Emission Properties of Phosphors for High Temperature Sensor Applications, 1988 IEEE Southeastcon, (88CH2571-8) pp. 228-233 (1988).

[5] H.Kusama, et al., Japanese J. of Appl. Physics, Vol. 15, No. 12, pp. 2349-2358 (1976).

[6] C.O.Egalon andR.S.Rogowski, Optical Engineering,vol. 31, no. 4, p.846 (1992).

[7] S.Albin, A.L.Briant, C.O.Egalon, R.S.Rogowski and J.S.Namkung, SPIE Proceedings, Chemical, Biological and Environmental Fiber Sensors, vol.1796, p. 393 (1992).

[8] A.A.Kaminskii and B.A.A.Antipenko, Multi-level Operating Schemes of Crystalline Lasers, Nauka Publishers, Moscow (1982) in Russian.

[9] N.C.Chang and J.B.Gruber, J. Chem. Phys., vol. 41, no. 10, pp.3227-3234 (1964).

[10] G.S.Ofelt, J. Chem.Phys., vol. 38, no. 9, pp. 2171-2180 (1962).

[11] D.B.M. Klassen, R.A.M. van Ham, and T.G.M. van Rijn, J. Luminescence, v. 43,pp. 261-274 (1989).

[12] M.S.Elmanharawy, A.H.Eid and A.A.Kader, Czech. J. Phys. B, vol. 28, pp. 1164-1173 (1978).

[13] C.W.Struck and W.H. Fonger, Understanding Luminescence Spectra and Efficiency Using Wp and Related Functions, Springer-Verlag, Berlin, Heidelberg (1991).

[12] D.E.McCumber and M.D.Sturge, J. Appl. Physics, Vol. 34, p. 1682 (1963).

[13] M.W.Yen, W.C.Scott, A.I.Schawlow, Phys. Rev., Vol. 136, p. A271 (1964).

[14] C.E.Byvik and A.M.Buoncristiani, IEEE J. of Quantum Electronics, Vol. QE-21, No. 10, pp.1619-24 (1985).

[15] A.M.Buoncristiani, C.E.Byvik and B.T.Smith, J. Appl. Physics, Vol. 53, No. 8, p. 5382-5386, (1982).

[16] W.M.Yen, Laser Spectroscopy of Solids II, Springer-Verlag, Berlin, Heidelberg (1989) J. M.Hollas, High Resolution Spectroscopy, Butterworths, London (1982).